Magneto-optical absorption of polarons

F. M. Peeters and J. T. Devreese*
Department of Physics, University of Antwerp, Universitaire Instelling Antwerpen, Universiteitsplein 1, B-2610 Wilrijk (Antwerpen), Belgium
(Received 21 April 1986)

The linear magneto-optical absorption of a polaron is derived for the Faraday (active and inactive mode) and the Voigt configurations. Our calculation is intended to be valid for arbitrary electron-phonon coupling constant, temperature, and magnetic fields. We start from the Kubo formula for the frequency-dependent conductivity and show that the essential quantity which we have to calculate is the electron density-density correlation function. This function is obtained by using the anisotropic Feynman polaron model. At zero magnetic field our result reduces to the optical absorption corresponding to the Feynman-Hellwarth-Iddings-Platzman approximation for a Fröhlich polaron, as derived by Devreese *et al.* [Phys. Rev. B 5, 2367 (1972)]. For small electron-phonon coupling the perturbation result is reobtained. Special attention is paid to the effect of the polaron instability [F.M. Peeters and J. T. Devreese, Phys. Rev. B 25, 7302 (1982)] on the magneto-optical absorption spectrum.

I. INTRODUCTION

The static properties of bulk polarons in a magnetic field have been extensively studied.[1-9] Especially the polaron ground-state energy and the effective mass at zero temperature were the object of study. A limited number of authors[1,8,9] have discussed the temperature (T) dependence of these quantities. From these studies elementary information can be obtained about the magneto-optical absorption spectrum of the polaron, e.g., for weak magnetic fields the inverse of the polaron mass determines the position of the cyclotron resonance line.

In the present paper we calculate the complete magneto-optical absorption spectrum of the polaron. This amounts to calculate a *dynamical* correlation function, namely, the velocity-velocity correlation function. Our approach relies on a generalization[9] of the Feynman description of the polaron[10] and is applicable for all values of the electron-phonon coupling strength, temperature and magnetic field strength.

Most of the earlier studies[11-25] on the magneto-optical absorption spectrum are restricted to the limit of weak electron-phonon coupling (α). These results rely on second-order perturbation theory. A nonperturbative approach was introduced by Thornber,[26,27] who constructed a self-consistent theory for the response of a polaron in combined electric and magnetic fields. This theory is based on a double path-integral formalism in which, after the exact elimination of the electron-phonon coordinates, the exact polaron evolution is simulated by a general quadratic action which has the same response as the approximate polaron response calculated in this way. The latter condition gives the self-consistency. No numerical solution of this self-consistent approach is known so far. Recently Saitoh[28] reobtained the results of Ref. 26 in the limit of vanishing external electric field by using a single path-integral formalism. This was accomplished by starting from the path-integral representation of the polaron free energy, where a driving force was introduced into the action. The response to this driving force then leads to the magneto-optical absorption spectrum. Analytic results were given in Ref. 28 for limiting values of α, T, $\mathscr{H}$ (magnetic field), and the frequency of the (vanishing) driving force. No numerical analysis was presented.

The present paper is organized as follows. In Sec. II the magneto-optical absorption is expressed in terms of a memory function. In order to do so we will use the Mori-Zwanzig projection operator technique.[29] This section generalizes Ref. 30 in which the path-integral result for the Feynman-Hellwarth-Iddings-Platzman (FHIP) (Refs. 31-33) polaron impedance function was reobtained by using operator techniques only. The memory function is calculated in Sec. III. The basic quantity in the memory function is the space Fourier transform of the electron density-density correlation function which is calculated within the anisotropic Feynman polaron model.[9] We show that our result for the magneto-optical absorption reduces to the optical absorption corresponding to the FHIP approximation as obtained in Ref. 33 in the limit of zero magnetic field. For weak electron-phonon coupling the result of Refs. 21 and 25 is reobtained. In Sec. IV numerical results are given for $T=0$, and different values of α and $\omega_c/\omega_{\rm LO}$ (ω_c is the free-electron cyclotron resonance frequency and $\omega_{\rm LO}$ is the LO-phonon frequency). The magneto-optical absorption spectrum is carefully studied for the value of α and $\omega_c/\omega_{\rm LO}$ at which, for the Feynman model in a magnetic field, a polaron instability was found in Ref. 9. The possible polaron instability was interpreted in Ref. 9 as a transition from a polaron state (polaron = electron + phonon cloud) to a state in which, in the direction perpendicular to the magnetic field, the polaron has lost its virtual phonon cloud. Our numerical results indicate that at the transition point the magneto-optical absorption spectrum changes drastically. Limitations of our approach are indicated and discussed. The conclusions are presented in Sec. V. Appendix A contains detailed formulas for the different memory functions (Voigt and Faraday configurations). The corresponding results for $\alpha \ll 1$ are listed in Appendix B. For conveni-

ence we use units such that $\hbar=\omega_{LO}=m=1$ (m is the electron band mass).

II. FORMULATION OF THE PROBLEM IN TERMS OF MEMORY FUNCTIONS

A polaron in a magnetic field is described by the Fröhlich Hamiltonian

$$H=\frac{1}{2m}\left[\mathbf{p}+\frac{e}{c}\mathbf{A}\right]^2+\sum_{\mathbf{k}}\hbar\omega_{\mathbf{k}}(a_{\mathbf{k}}^{\dagger}a_{\mathbf{k}}+\tfrac{1}{2}) + \sum_{\mathbf{k}}(V_{\mathbf{k}}a_{\mathbf{k}}e^{i\mathbf{k}\cdot\mathbf{r}}+V_{\mathbf{k}}^{*}a_{\mathbf{k}}^{\dagger}e^{-i\mathbf{k}\cdot\mathbf{r}}) , \tag{1}$$

where we used the standard notations. The magnetic field ($\mathscr{H}$) will be chosen along the z axis and the vector potential is expressed in the symmetrical Coulomb gauge $\mathbf{A}=\mathscr{H}/2\,(-y,x,0)$. The frequency-dependent magneto-optical absorption is given by

$$\mu(\omega)=\mathrm{Re}\left[\frac{1}{Z(\omega)}\right] \tag{2}$$

with the inverse of the impedance function

$$\frac{1}{Z(\omega)}=ie\lim_{\epsilon\to+0}\Phi(\omega+i\epsilon) \tag{3}$$

and the relaxation function[34] ($z=\omega+i\epsilon$, $\epsilon>0$)

$$\Phi(z)=\left[A,\frac{1}{z-L}A\right] =-i\int_0^{\infty}dt\,e^{izt}\int_0^{\beta}d\lambda\langle A^{\dagger}(t-i\lambda)A(0)\rangle , \tag{4}$$

where A is the velocity operator, $\beta=1/k_BT$, L is the Liouville operator with $LA=[H,A]$, $A(t)=e^{iLt}A(0)$, and $\langle\cdots\rangle$ is a thermal average. Three independent configurations are of interest.

(i) $A=\dot{z}$, which is called the *Voigt configuration*. The corresponding relaxation function is denoted by $\Phi_{zz}(z)$ and gives the linear response to an oscillating electric field parallel to the magnetic field.

(ii) $A=\dot{x}+i\dot{y}$ gives the *Faraday configuration* for the cyclotron resonance *active mode*. The relaxation function in this case $\frac{1}{2}\Phi_{+}(z)$ describes the response to circular polarized light along the z axis (which leads to an oscillating electric field perpendicular to the $\mathscr{H}$ field).

(iii) $A=\dot{x}-i\dot{y}$ leads to the *Faraday configuration* for the cyclotron *inactive mode*. In this case the relaxation function is given by[35,36]

$$\phi_{-}(z)=-[\Phi_{+}(-z^{*})]^{*}=-\Phi_{+}(-z) .$$

Using the Mori-Zwanzig projection operator techniques one can write Eq. (4) as

$$\Phi(z)=\frac{\chi}{z-\Omega-\Sigma(z)} , \tag{5}$$

with the static correlation functions

$$\chi=(A,A) , \qquad \Omega=(A,LA)\chi^{-1} , \tag{6}$$

and the memory function

$$\Sigma(z)=\left[QLA,\frac{1}{z-QLQ}QLA\right]\chi^{-1} , \tag{7}$$

where P ($Q\equiv1-P$) is the projection operator on the operator variable A

$$PB=A(A,B)\chi^{-1} , \tag{8}$$

with B another variable. The new Liouville operator $\mathscr{L}=QLQ$ describes the time evolution in the Hilbert space of operators which is orthogonal to A.

For the above three situations we have the following.

(i) $A=\dot{z}$ gives us

$$\chi=1/m, \quad \Omega=0 , \qquad \Sigma_{zz}(z)=\frac{1}{m}\sum_{\mathbf{k}}k_z^2\,|\,V_{\mathbf{k}}\,|^2[\Phi_{\mathbf{k}}^{++}(z)+\phi_{\mathbf{k}}^{--}(z)+\Phi_{\mathbf{k}}^{+-}(z)+\phi_{\mathbf{k}}^{-+}(z)] , \tag{9}$$

with

$$\Phi_{\mathbf{k}}^{++}(z)=\left[b_{\mathbf{k}}^{\dagger},\frac{1}{z-\mathscr{L}}b_{\mathbf{k}}^{\dagger}\right] , \tag{10a}$$

$$\Phi_{\mathbf{k}}^{+-}(z)=\left[b_{\mathbf{k}}^{\dagger},\frac{1}{z-\mathscr{L}}b_{\mathbf{k}}\right] , \tag{10b}$$

$$\Phi_{\mathbf{k}}^{--}(z)=-[\Phi_{-\mathbf{k}}^{++}(-z^{*})]^{*} , \tag{10c}$$

$$\Phi_{\mathbf{k}}^{-+}(z)=-[\Phi_{-\mathbf{k}}^{+-}(-z^{*})]^{*} , \tag{10d}$$

where $b_{\mathbf{k}}=a_{\mathbf{k}}e^{i\mathbf{k}\cdot\mathbf{r}}$.

(ii) $A=\dot{x}+i\dot{y}$ gives us

$$\chi=2/m, \quad \Omega=\omega_c , \qquad \Sigma_{+}(z)=\Sigma(z)-\tfrac{1}{2}\Sigma_{zz}(z) , \tag{11}$$

$$\Sigma(z)=\frac{1}{2m}\sum_{\mathbf{k}}k^2\,|\,V_{\mathbf{k}}\,|^2[\Phi_{\mathbf{k}}^{++}(z)+\Phi_{\mathbf{k}}^{--}(z)+\Phi_{\mathbf{k}}^{+-}(z)+\Phi_{\mathbf{k}}^{-+}(z)] . \tag{12}$$

(iii) $A=\dot{x}-i\dot{y}$ gives us

$$x=2/m, \quad \Omega=-\omega_c , \qquad \Sigma_{-}(z)=-\Sigma_{+}(-z) . \tag{13}$$

III. CALCULATION OF THE MEMORY FUNCTION USING THE ANISOTROPIC FEYNMAN POLARON MODEL

The basic quantities in the memory functions $\Sigma_{zz}(z)$, $\Sigma(z)$ are the relaxation functions $\Phi_{\mathbf{k}}^{++}(z)$ and $\Phi_{\mathbf{k}}^{+-}(z)$ [see Eqs. (10a)–(10d)]. Therefore we consider

$$\Phi_{\mathbf{k}}^{++}(z)=-i\int_0^{\infty}dt\,e^{izt}(b_{\mathbf{k}}^{\dagger}(t),b_{\mathbf{k}}^{\dagger}(0)) , \tag{14}$$

which, after a partial integration, can be reduced to

$$\Phi_{\mathbf{k}}^{++}(z)=\frac{i}{z}\int_0^{\infty}dt(1-e^{izt})\langle[b_{\mathbf{k}}(t),b_{\mathbf{k}}^{\dagger}(0)]\rangle . \tag{15}$$

A similar calculation for $\Phi_{\mathbf{k}}^{+-}(z)$ shows that the memory functions can be written as

$$\Sigma_{zz}(z)=\frac{1}{m}\sum_{\mathbf{k}}k_z^2\,|\,V_{\mathbf{k}}\,|^2F_{\mathbf{k}}(z)\ , \tag{16a}$$

$$\Sigma(z)=\frac{1}{m}\sum_{\mathbf{k}}k^2\,|\,V_{\mathbf{k}}\,|^2F_{\mathbf{k}}(z)\ , \tag{16b}$$

with

$$F_{\mathbf{k}}(z)=-\frac{2}{z}\int_0^\infty dt(1-e^{izt})\mathrm{Im}\langle[b_{\mathbf{k}}(t),b_{\mathbf{k}}^\dagger(0)]+[b_{\mathbf{k}}(t),b_{\mathbf{k}}(0)]\rangle\ . \tag{17}$$

In an earlier publication[30] we showed, in the case of zero magnetic field, how to approximate the correlation functions (e.g., $\langle b_{\mathbf{k}}(t)b_{\mathbf{k}}^\dagger(0)\rangle$) in order to obtain the FHIP result.[31] Here we will proceed in the same way as in Ref. 30 and replace $\mathscr{L}$ by $L_{\mathrm{ph}}+L_F$, with L_{ph} the Liouville operator for free phonons and L_F the Liouville operator for the anisotropic two-particle Feynman polaron model, respectively. With this approximation we obtain

$$\langle b_{\mathbf{k}}(t)b_{\mathbf{k}}^\dagger(0)\rangle=\langle a_{\mathbf{k}}(t)a_{\mathbf{k}}^\dagger(0)\rangle\langle e^{i\mathbf{k}\cdot\mathbf{r}(t)}e^{-i\mathbf{k}\cdot\mathbf{r}(0)}\rangle\ , \tag{18}$$

where

$$\langle a_{\mathbf{k}}(t)a_k^\dagger(0)\rangle=[1+n(\omega_{\mathbf{k}})]e^{-i\omega_{\mathbf{k}}t}\ ,$$

with

$$n(\omega_{\mathbf{k}})=1/(e^{\beta\omega_{\mathbf{k}}}-1)$$

the number of phonons with frequency $\omega_{\mathbf{k}}$ and

$$\langle e^{i\mathbf{k}\cdot\mathbf{r}(t)}e^{-i\mathbf{k}\cdot\mathbf{r}(0)}\rangle=S^*(-\mathbf{k},t)\ ,$$

where $S(\mathbf{k},t)$ is the space Fourier transform of the electron density-density correlation function. $S(\mathbf{k},t)$ for an electron described by the anisotropic Feynman polaron model has been calculated in Ref. 9 and is given by

$$S(\mathbf{k},t)=e^{-k_z^2D(t)}e^{-k_\perp^2D_H(t)}\ , \tag{19}$$

with $k_\perp^2=k_x^2+k_y^2$;

$$D(t)=\frac{1}{2M_{\|}}\left[-it+\frac{t^2}{\beta}\right]+d_0^2\left[1-e^{is_0t}+4n(s_0)\sin^2\left[\frac{s_0t}{2}\right]\right]\ , \tag{20a}$$

$$D_H(t)=\sum_{j=1}^{3}d_j^2\left[1-e^{is_jt}+4n(s_j)\sin^2\left[\frac{s_jt}{2}\right]\right]\ , \tag{20b}$$

where $M_{\|}=(v_{\|}/w_{\|})^2$ is the mass of the Feynman polaron model along the magnetic field,

$$d_0^2=(v_{\|}^2-w_{\|}^2)/2v_{\|}^3\ ,$$

$$d_j^2=(s_j^2-w_\perp^2)/2s_j[3s_j^2+2(-1)^j\omega_cs_j-v_\perp^2]$$

for $j=1,2,3$. $s_0=v_{\|}$ and $s_1\le s_2\le s_3$ are given by the positive roots of the equation

$$s_j^2(s_j^2-v_\perp^2)^2-\omega_c^2(s_j^2-w_\perp^2)^2=0\ .$$

The parameters for the anisotropic Feynman model $v_{\|},w_{\|},v_\perp,w_\perp$ have been determined in Ref. 9 on the basis of Feynman's conjecture that the variational principle for path integrals for the polaron free energy remains valid in the presence of a magnetic field. Recently Larsen[37] has questioned the variational character of the free energy of a polaron in a magnetic field as calculated in Ref. 9 for the case of a polaron in two dimensions.[38]

For a polaron one has $\omega_{\mathbf{k}}=\omega_{\mathrm{LO}}$, $|\,V_{\mathbf{k}}\,|^2=2\sqrt{2}\pi\alpha/k^2V$ (with V the volume of the crystal) and, with the above approximations, we obtain for the memory functions

$$\Sigma_{zz}(z)=\frac{2}{z}\int_0^\infty dt(1-e^{izt})\mathrm{Im}G_{zz}(t)\ , \tag{21a}$$

$$\Sigma(z)=\frac{2}{z}\int_0^\infty dt(1-e^{izt})\mathrm{Im}G(t)\ , \tag{21b}$$

with

$$G_{zz}(t)=\frac{\alpha}{4\sqrt{2\pi}}F(t)\left[\frac{1}{H(t)^{3/2}}\ln\left[\frac{\sqrt{D(t)}+\sqrt{H(t)}}{\sqrt{D(t)}-\sqrt{H(t)}}\right]-\frac{2}{\sqrt{D(t)}H(t)}\right]\ , \tag{22a}$$

$$G(t)=\frac{\alpha}{4\sqrt{2\pi}}\frac{F(t)}{\sqrt{D(t)}D_H(t)}\ , \tag{22b}$$

where

$$H(t)=D(t)-D_H(t)\ , \tag{23a}$$

$$F(t)=(1+N)e^{i\omega t}+Ne^{-i\omega t}\ , \tag{23b}$$

and $N=n(\omega_{\mathrm{LO}})$ is the number of LO phonons.

In Ref. 9 we showed that in the limit of zero magnetic field $D_H(t)\to D(t)$ and correspondingly $G(t)\to\frac{3}{2}G_{zz}(t)$. This implies

$$\Sigma_+(z)\to\Sigma_{zz}(z)=\frac{\alpha}{3\sqrt{2\pi}}\int_0^\infty dt\frac{1-e^{izt}}{z}\mathrm{Im}\left[\frac{F(t)}{[D(t)]^{3/2}}\right]$$

which is the result[30] of FHIP.

IV. NUMERICAL ANALYSIS

In order to obtain numerical results for the polaron magneto-optical absorption spectrum [see Eqs. (3) and (5)] we compute the memory functions [(21a) and (21b)]. The integrand of the integrals of Eqs. (21a) and (21b) consist of a factor which decreases slowly when $t\to\infty$ (i.e., $t^{-\delta}$ with $\delta\gtrsim1$ for $t\to\infty$) superimposed on a rapidly oscillating component. As a consequence this representation for the memory functions $\Sigma(z)$ and $\Sigma_{zz}(z)$ is not suitable for numerical programming. Furthermore $\Sigma(z)$ and $\Sigma_{zz}(z)$ shows some divergences, which are not directly apparent from Eqs. (21a) and (21b). In order to circumvent these

difficulties we present in Appendix A another representation of Eqs. (21a) and (21b) which, although it results in more intricate expressions, it is more suitable for numerical work. The divergent behavior of $\Sigma(z)$ and $\Sigma_{zz}(z)$ for certain ω values ($z=\omega+i\epsilon$), can be subtracted in the representation of Appendix A explicitly.

In Appendix B it is shown that in the small coupling limit our results reduce to the results of Ref. 25. A significant simplification is obtained within the present formulation: in Ref. 25 the memory function was represented as a fivefold series while in Appendix B we were able to reduce this expression to a twofold series. We refer to Refs. 21, 23, and 25 for numerical results in the limit $\alpha \ll 1$ (the numerical results of Ref. 25 correspond to the case of InSb which has $\alpha=0.02$).

The magneto-optical absorption spectrum in the *Faraday (active-mode)* configuration (this is the configuration in which the cyclotron resonance experiments are performed) is given by

$$-\frac{1}{2}\frac{\mathrm{Im}\Sigma_+(\omega)}{[\omega-\omega_c-\mathrm{Re}\Sigma_+(\omega)]^2+[\mathrm{Im}\Sigma_+(\omega)]^2}\ . \tag{24}$$

For $\omega_c=0$, Eq. (24) reduces to the expression (11a) of Ref. 33. The expressions for the real and imaginary part of the memory function $\Sigma_+(\omega)=\Sigma(\omega)-\frac{1}{2}\Sigma_{zz}(\omega)$ are given in Appendix A. A numerical analysis of expression (24) leads to the results shown in Fig. 1 for $\alpha=1$ and in Fig. 2 for $\alpha=3$. In these figures the magneto-optical absorption is plotted as a function of the frequency of the incident radiation for different values of the magnetic field. When $\omega<\omega_{\mathrm{LO}}$ the imaginary part of the memory function is zero and therefore the magneto-optical absorption will also be zero except for these frequencies for which

$$\omega-\omega_c-\mathrm{Re}\Sigma_+(\omega)=0\ , \tag{25}$$

at which Eq. (24) becomes a δ function. For $\omega<\omega_{\mathrm{LO}}$ Eq. (25) has only one solution $\omega=\omega_c^*$ which determines the position of the cyclotron resonance peak. It is standard practice to define a cyclotron mass

$$\frac{m^*}{m_b}=\frac{\omega_c}{\omega_c^*} \tag{26}$$

which is magnetic field dependent. Figure 3 gives the magnetic field dependence of the polaron cyclotron mass for different values of α which are in the range of values typical for most common ionic crystals. In the zero magnetic field limit the definition (26) for the polaron cyclotron mass leads to a mass which is identical to the polaron mass as calculated by Feynman[10] if ω_c^* in Eq. (26) is given by the zero of Eq. (25), $\omega=\omega_c^*$.

From Fig. 3 it is apparent that the polaron mass increases with increasing magnetic field and that the mass increase is larger for larger electron-phonon coupling. In a recent paper[39] we compared different theories for the calculation of the polaron cyclotron mass and found that calculations which are based on second-order perturbation theory [e.g., improved Wigner Brillouin perturbation theory[40] (IWBPT)] can give accurate values for the cyclotron mass (within 10%) for $\alpha<0.1$. For larger values of α IWBPT appreciably underestimates the polaron correction to the cyclotron mass.

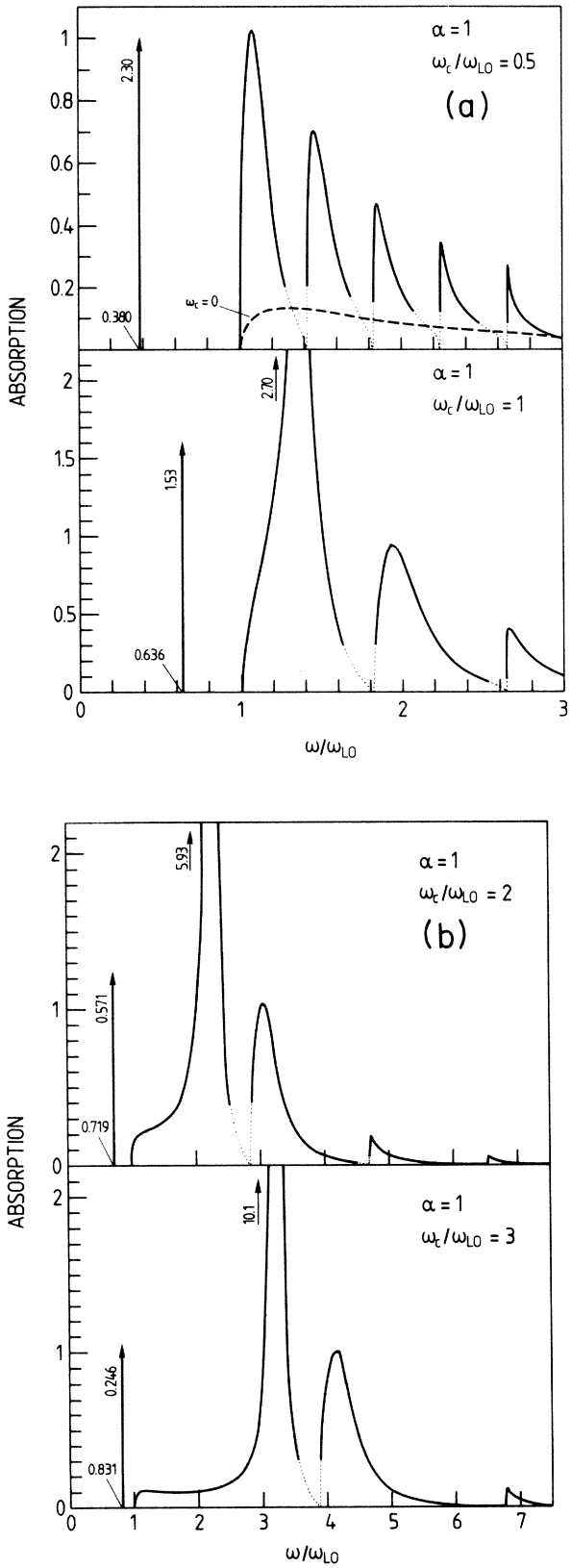

FIG. 1. Polaron magneto-optical absorption in the Faraday active-mode configuration for $\alpha=1$, $T=0$, and five different values of the magnetic field. The present approximation is not valid where the magneto-optical absorption is represented by points.

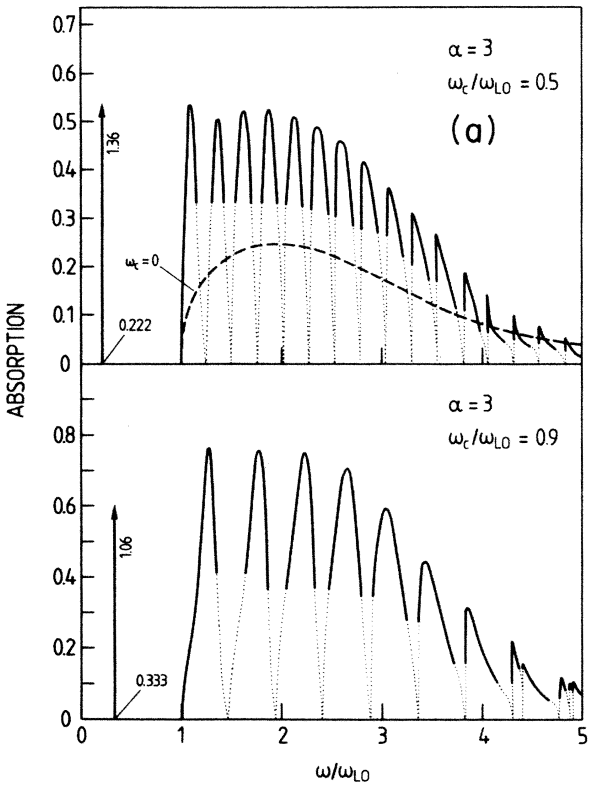

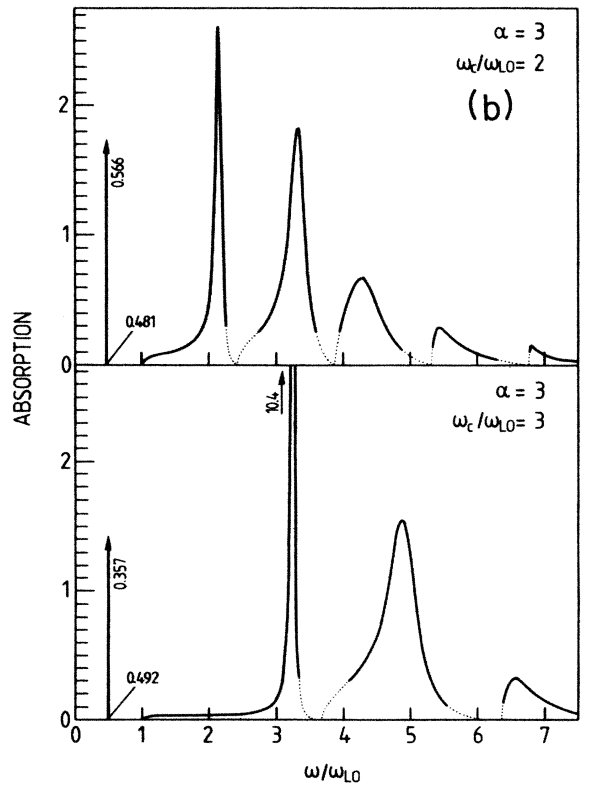

FIG. 2. Same as Fig. 1, but now for $\alpha=3$.

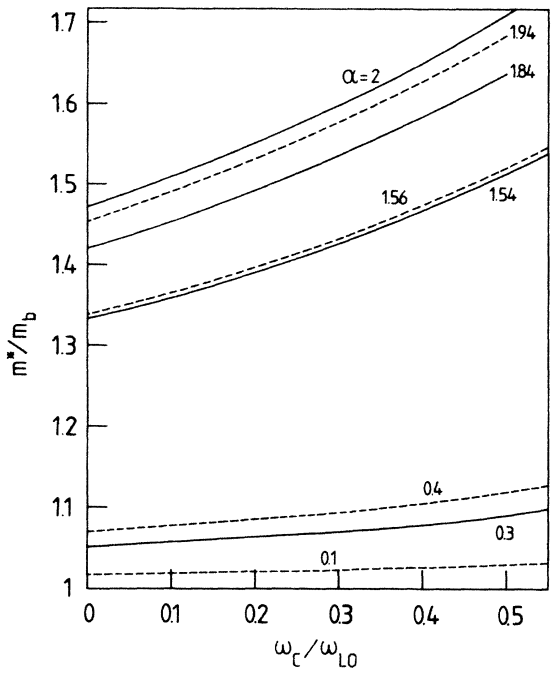

FIG. 3. Magnetic field dependence of the polaron cyclotron mass for different values of the electron-phonon coupling constant.

For a comparison of the polaron cyclotron mass obtained with the present theory with experimental cyclotron resonance data we refer to Ref. 41 for the material CdTe (Ref. 42) and to Ref. 43 for AgBr and AgCl. In those references new values for the electron band mass and electron-phonon coupling constant are obtained. The present theory incorporates the polaron effects more completely (i.e., beyond second-order perturbation theory); the polaron corrections to the cyclotron mass are found to be larger accordingly. As a consequence we found that (i) the electron band mass determined from a comparison with experimental cyclotron resonance data is smaller and (ii) also the electron-phonon coupling constant is slightly smaller than found with other theories.

Within the present approach (in which collisional broadening is not included) we find that for $T=0$ the cyclotron resonance peak is a delta function. In Figs. 1 and 2 the position of this δ function is indicated by a vertical arrow. The oscillator strength of this peak

$$\pi\left|1-\frac{\partial}{\partial\omega}\mathrm{Re}\Sigma_+(\omega)\right|^{-1}_{\omega=\omega_c^*} \tag{27}$$

is also indicated in the figures. With increasing magnetic field the oscillator strength of the cyclotron resonance peak decreases and is transferred to the peaks in the continuum which occur for $\omega>\omega_{\mathrm{LO}}$. In the limit $\omega_c\to\infty$ we found that the oscillator strength of the cyclotron resonance peak approaches zero and the position $\omega_c^*\to\omega_{\mathrm{LO}}$. This is illustrated in Fig. 4 for $\alpha=1$ and in Fig. 5 for $\alpha=3$ where the position of the first five peaks in the spectrum are plotted as a function of the magnetic field. In the small magnetic field limit, i.e., $\omega_c\ll\omega_{\mathrm{LO}}$, a cyclotron

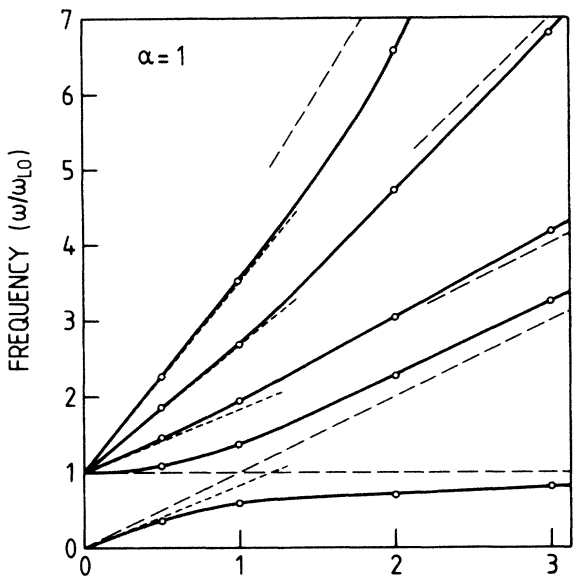

FIG. 4. Position of the different peaks in the cyclotron resonance spectrum for $\alpha=1$ and $T=0$. (Solid curves are guides to the eye.) The dashed curves for $\omega_c/\omega_{\rm LO}<1.5$ represent the energies $\hbar\omega_c^*$ and $\hbar\omega_{\rm LO}+n\hbar\omega_c^*$, with $n=0,1,2,3$. For $\omega_c/\omega_{\rm LO}>1.5$ the dashed curves show ω_c and $\omega_{\rm LO}+n\omega_c$, with $n=0,1,2,3$.

resonance peak occurs at $\omega_c^*=(m_b/m^*)\omega_c<\omega_c$ and a series of peaks are found with frequency $\omega_{\rm LO}+n\omega_c^*$, where $n=0,1,2,\ldots$. The dashed lines for $\omega_c/\omega_{\rm LO}<1.5$ in Figs. 4 and 5 indicate the limiting behavior (i.e., $\omega_c\to 0$) of the position of these peaks. The peaks in the continuum at $\omega\sim\omega_{\rm LO}+n\omega_c^*$ correspond to transition from the ground-state Landau level to the nth Landau level with, at the same time, emission of a LO phonon. Most of the oscillator strength is contained in the cyclotron resonance peak if $\omega_c\ll\omega_{\rm LO}$. In the high magnetic field limit a peak occurs at $\omega\sim\omega_c$ together with a series of peaks around $\omega\simeq\omega_{\rm LO}+n\omega_c$, $n=0,1,2,\ldots$. For $\omega_c/\omega_{\rm LO}>1.5$ dashed straight lines are drawn in Figs. 4 and 5 corresponding to $\omega=\omega_c$ and $\omega=\omega_{\rm LO}+n\omega_c$, $n=0,1,2,\ldots$. Most of the oscillator strength is now contained in the peak with frequency ω_c. For $\alpha>1$ the large magnetic field behavior of the side peaks is only very roughly approximated by $\omega_{\rm LO}+n\omega_c$. A possible reason is that the Landau levels become mixed with the internal relaxed excited polaron states[33] which complicates the picture considerably.

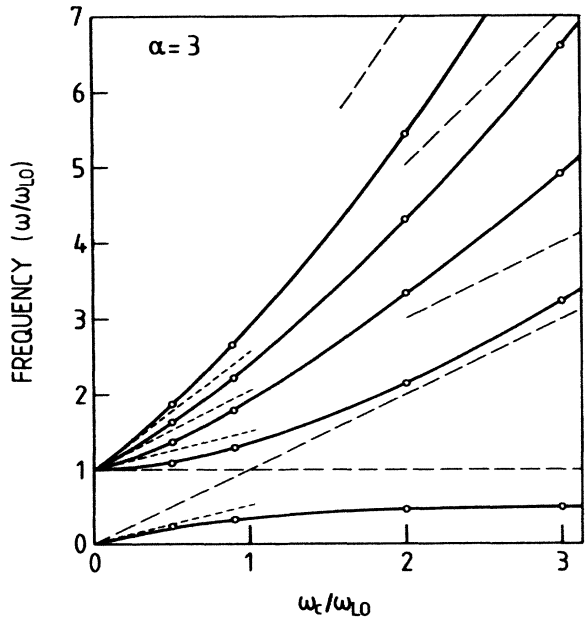

FIG. 5. Same as Fig. 4 but now for $\alpha=3$.

In Figs. 1 and 2 the magneto-optical absorption becomes zero for certain values of the magnetic field. This is due to an artefact of the present approximation as will be discussed at the end of this section. The part of the magneto-optical absorption spectrum drawn as a point line in Figs. 1 and 2 corresponds with the region where the present approximation is invalid.

The magneto-optical absorption in the Faraday *inactive-mode* configuration

$$-\frac{1}{2}\frac{\mathrm{Im}\Sigma_-(\omega)}{[\omega+\omega_c-\mathrm{Re}\Sigma_-(\omega)]^2+[\mathrm{Im}\Sigma_-(\omega)]^2} \tag{28}$$

is shown in Fig. 6 for $\alpha=1$ and for three values of the magnetic field, $\omega_c/\omega_{\rm LO}=0.5,1,2$. From Appendix A, Eq. (A7), we know that $\Sigma_\pm(z)=\Sigma_\pm^M(z)-\Sigma_\pm^M(-z)$ which results in

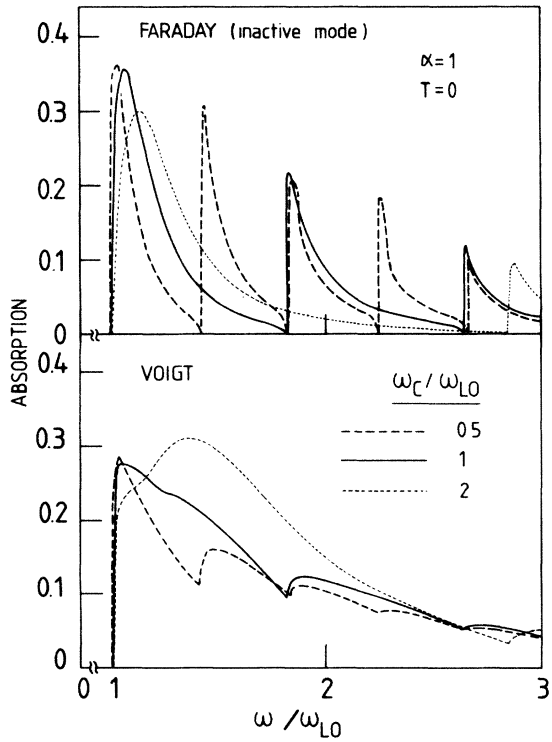

FIG. 6. Magneto-optical absorption spectrum for polarons: (i) in the Faraday inactive-mode configuration (upper part of figure) and (ii) in the Voigt configuration (lower part of figure) for $\alpha=1$, $T=0$, and for three values of the magnetic field.

$$\mathrm{Re}\Sigma_{\pm}(\omega)=\mathrm{Re}\Sigma^{M}_{\pm}(\omega)-\mathrm{Re}\Sigma^{M}_{\pm}(-\omega)=-\mathrm{Re}\Sigma_{\pm}(-\omega)$$

and

$$\mathrm{Im}\Sigma_{\pm}(\omega)=\mathrm{Im}\Sigma^{M}_{\pm}(\omega)+\mathrm{Im}\Sigma^{M}_{\pm}(-\omega)=\mathrm{Im}\Sigma_{\pm}(-\omega)\ .$$

When we combine these properties with Eq. (13) we find

$$\mathrm{Re}\Sigma_{-}(\omega)=-\mathrm{Re}\Sigma_{+}(-\omega)=\mathrm{Re}\Sigma_{+}(\omega)=\mathrm{Re}\Sigma_{\perp}(\omega)\ , \quad (29a)$$

$$\mathrm{Im}\Sigma_{-}(\omega)=\mathrm{Im}\Sigma_{+}(-\omega)=\mathrm{Im}\Sigma_{+}(\omega)=\mathrm{Im}\Sigma_{\perp}(\omega)\ , \quad (29b)$$

and as a result the real and imaginary part of the memory function are the same in the Faraday active- and in the Faraday inactive-mode configuration. The only difference is the sign in front of ω_c. If we compare the magneto-optical absorption spectrum of Fig. 6 (Faraday inactive-mode configuration) with the one in Fig. 1 we notice the following differences: (i) the magneto-optical absorption is weaker in the Faraday inactive-mode configuration, (ii) there is no absorption for $\omega<\omega_{\mathrm{LO}}$, and no cyclotron resonance peak is present in the Faraday inactive mode, and (iii) in the Faraday inactive mode a peak occurs at a frequency just above the LO-phonon frequency; its position depends only weakly on the magnetic field strength. For frequencies above threshold (i.e., $\omega>\omega_{\mathrm{LO}}$) the magneto-optical absorption spectrum is very similar to the magneto-optical absorption spectrum of the Faraday active-mode configuration. This can easily be understood because for sufficiently high frequencies the magneto-optical absorption spectrum is given by $-\frac{1}{2}\mathrm{Im}\Sigma_{\perp}(\omega)/\omega^2$.

In the *Voigt* configuration the magnetic field is parallel to the oscillating electric field and the magneto-optical absorption spectrum is given by

$$\frac{-\mathrm{Im}\Sigma_{zz}(\omega)}{[\omega-\mathrm{Re}\Sigma_{zz}(\omega)]^2+[\mathrm{Im}\Sigma_{zz}(\omega)]^2} \quad (30)$$

which for $\alpha=1$ is plotted in the lower part of Fig. 6 for $\omega_c/\omega_{\mathrm{LO}}=0.5$, 1, and 2. Notice that the structure in the magneto-optical absorption spectrum is less pronounced in the Voigt configuration in comparison with the Faraday configuration. As $\omega_c=0$, both Eqs. (28) and (30) reduce to Eq. (11a) of Ref. 33.

In the following part of this section we will concentrate on the influence of the polaron instability as found in Ref. 9 on the magneto-optical absorption spectrum. As an example we take $\alpha=5$, $T=0$. In Ref. 9 it was found that for this value of the electron-phonon coupling strength the polaron state becomes unstable for $\omega_c/\omega_{\mathrm{LO}}=2.77$. At this instability point it was predicted[9] that the polaron system makes a transition (as a function of increasing magnetic field) from a *polaron state* (also called "dressed" state) to an *electron state* (also called "stripped" state) in a magnetic field. The transition dressed state→stripped state occurs in the direction perpendicular to the magnetic field. Parallel to the magnetic field no such transition takes place. In Ref. 9 we found that for the physical parameters $\alpha=5$, $T=0$, $\omega_c/\omega_{\mathrm{LO}}=2.77$ the parameters of the anisotropic Feynman polaron in the dressed state are $v_{\perp}=4.79$, $w_{\perp}=1.99$, $v_{\parallel}=4.27$, $w_{\parallel}=1.72$, which gives the eigenfrequencies $s_1=0.456$, $s_2=3.88$, and $s_3=6.19$; while for the stripped state one has $v_{\perp}=11.89$, $w_{\perp}=10.03$, $v_{\parallel}=4.07$, $w_{\parallel}=1.68$, which results in $s_1=1.95$, $s_2=11.55$, and $s_3=12.38$.

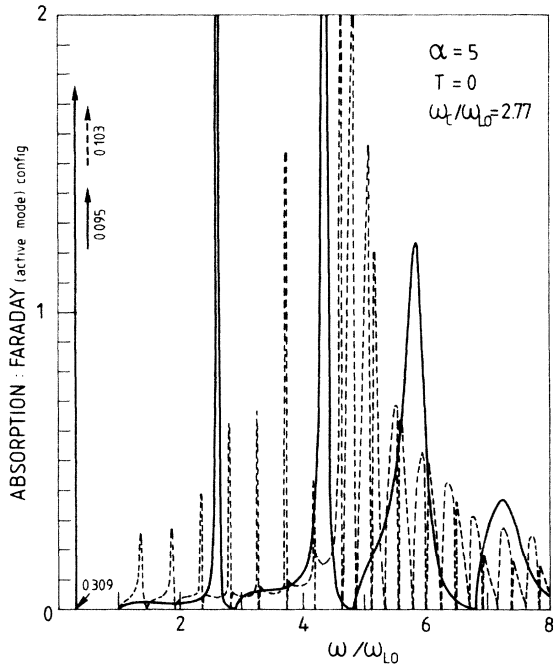

FIG. 7. Polaron magneto-optical absorption spectrum in the Faraday configuration at $T=0$ for the cyclotron resonance active mode. The electron-phonon coupling constant is $\alpha=5$ and the magnetic field is $\omega_c/\omega_{\mathrm{LO}}=2.77$. The solid curve indicates the magneto-optical absorption for the polaron in the stripped state while the dashed curve is the corresponding absorption for the dressed state. The cyclotron resonance peak is a delta function with weight 0.095 (0.103) when the polaron is in the dressed (stripped) state.

A zeroth-order calculation of the position and relative intensity (oscillator strength) of the first two peaks in the magneto-optical absorption spectrum was presented in an earlier publication.[44] Here we give numerical results for the complete spectrum using the more complete approach outlined in preceding sections.

The magneto-optical absorption spectrum in the Faraday active-mode configuration for $\alpha=5$ is plotted in Fig. 7 for the "dressed polaron state" (dashed curve) and for the "stripped state" (full curve). A similar result for the Faraday inactive-mode configuration is given in Fig. 8 for the same physical quantities. The present approximation is not valid close to the frequencies where the magneto-optical absorption becomes zero. For reasons of clarity we did not represent the absorption curve in this region by a point curve as in Figs. 1 and 2. The zeros in the spectra of Figs. 7 and 8 can be traced back to the divergent behavior of the memory function $\Sigma_{\perp}(\omega)$ for certain frequencies (see Fig. 9). The frequencies at which $\mathrm{Im}\Sigma_{\perp}(\omega)$ and $\mathrm{Re}\Sigma_{\perp}(\omega)$ are divergent can be obtained directly from the representation of the memory function presented in Appendix A. The expressions (A16) and (1.18) are divergent when

$$\omega/\omega_{\mathrm{LO}}-1-(n_0s_0+n_1s_1+n_2s_2+n_3s_3)=0$$

with

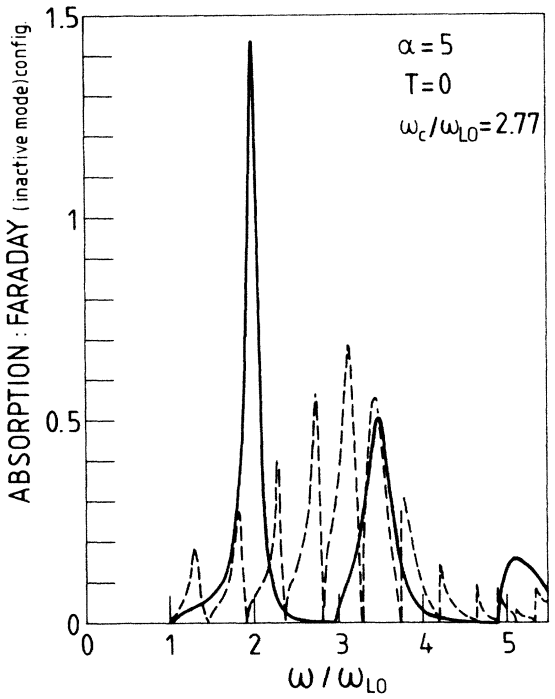

FIG. 8. Same as Fig. 7 but now for the cyclotron resonance inactive mode.

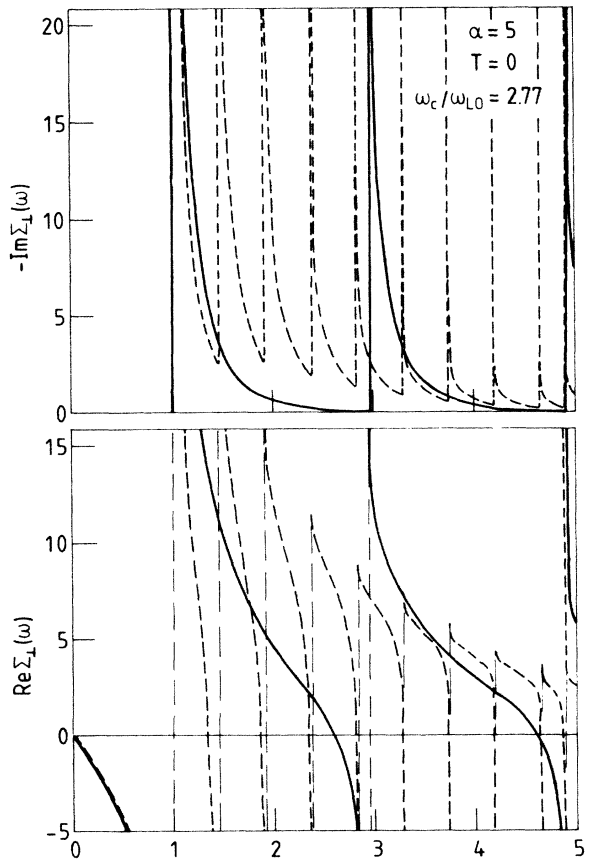

FIG. 9. Real and imaginary part of the memory function for the magneto-optical absorption spectrum in the Faraday configuration. Solid and dashed curves correspond to the same polaron state as in Fig. 7.

$n_0, n_1, n_2, n_3 = 0, 1, 2, \ldots$.

It is well known that the singularities in the memory function are an artefact of the present approximation and result from the singularities in the nonperturbated electron density of states. The density of states

$$n(E) = \frac{1}{V} \mathrm{Tr}\delta(E - H)$$

(V is the volume of the crystal) for the anisotropic Feynman polaron model in a magnetic field is

$$n(E) = \frac{m\omega_c}{(2\pi\hbar)^2} \sqrt{2m} \left[\frac{v_{\|}}{w_{\|}} \right] \times \sum_{n_\mu=0}^{\infty} \frac{\theta(E - E_0 - n_\mu s^\mu)}{(E - E_0 - n_\mu s^\mu)^{1/2}} , \tag{31}$$

with $E_0 = \frac{1}{2} \sum_{\mu=0}^{4} s^\mu$ the zero-point energy of this model system,

$$n_\mu s^\mu = \sum_{\mu=0}^{4} n_\mu s_\mu$$

and

$$\sum_{n_\mu=0}^{\infty} = \sum_{n_0=0}^{\infty} \sum_{n_1=0}^{\infty} \sum_{n_2=0}^{\infty} \sum_{n_3=0}^{\infty} .$$

The behavior of the density of states is shown in Fig. 10 for the case $\alpha = 5$, $T = 0$, $\omega_c/\omega_{LO} = 2.77$. The position of the divergencies in $n(E)$ coincides exactly with the divergencies in the real and imaginary part of the memory

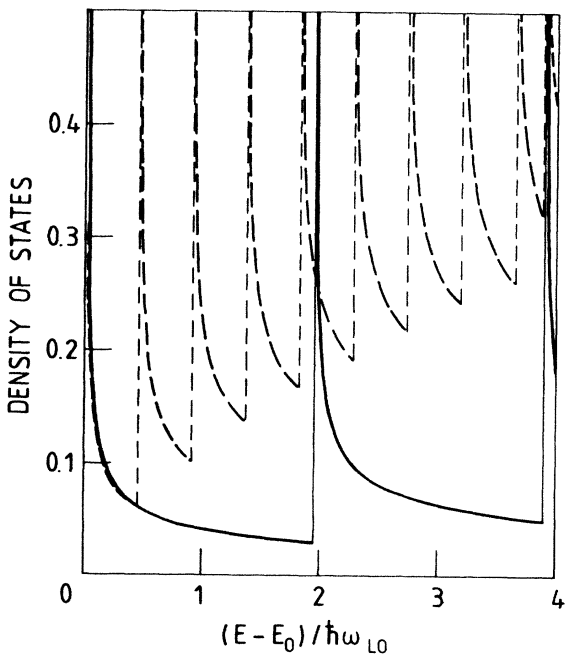

FIG. 10. Density of states for the anisotropic Feynman polaron model. E_0 is the zero-point energy of this model. Solid and dashed curves have the same meaning as in Fig. 7.

function $\Sigma_\perp(\omega)$ (see Fig. 9).

In a more complete theory one must take into account the broadening of the Landau levels due to the interaction between the electrons and the LO phonons or other scattering mechanisms like, e.g., acoustical phonons, impurities, etc. This will wash out the divergencies in the density of states which ultimately will result in the disappearance of the divergencies in the memory function and consequently in the disappearance of the spurious zeros in the calculated absorption spectrum in the case of the Faraday configuration.

The polaron magneto-optical absorption spectrum in the Voigt configuration is shown in Fig. 11 for the same physical parameters as in Fig. 7. In the Voigt configuration the spectrum does not exhibit any spurious zeros as in the case of the Faraday configuration. The reason is that the corresponding memory function $\Sigma_{zz}(z)=\Sigma_{||}(z)$ (see Fig. 12) does not have divergences like $\Sigma_\perp(z)$ does; this is because in the Voigt configuration no *direct* transition between the Landau levels is possible (the electric field is directed parallel to the magnetic field). Nevertheless, due to the spherical symmetrical nature of the electron-LO phonon coupling the mechanism which leads to the divergencies in $\Sigma_\perp(z)$ is still weakly present and leads to discontinuities in the derivative $\partial\Sigma_{||}(\omega)/\partial\omega$. Transitions between Landau levels are only possible with the mediation of a LO phonon in this case.

Now we turn to the discussion of the physical interpretation of Figs. 7, 8, and 11. It is remarkable that within the numerical accuracy the position of the cyclotron resonance peak (see Fig. 7) is the same in both polaron states;

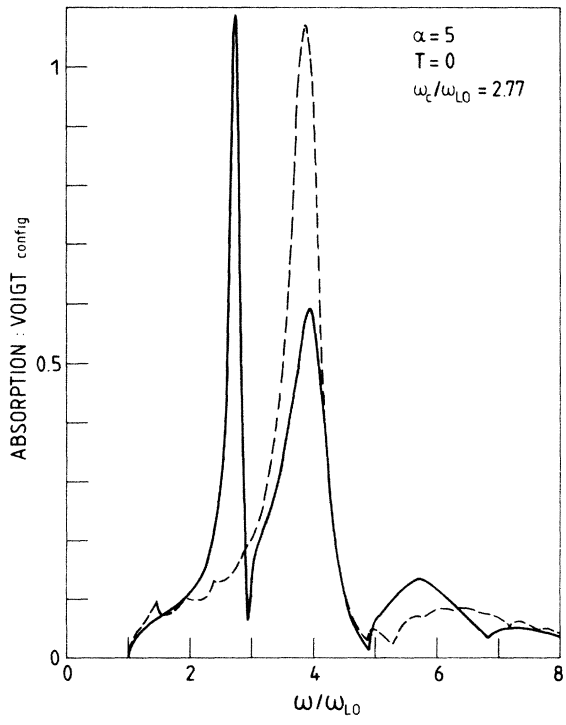

FIG. 11. Same as Fig. 7 but now for the Voigt configuration.

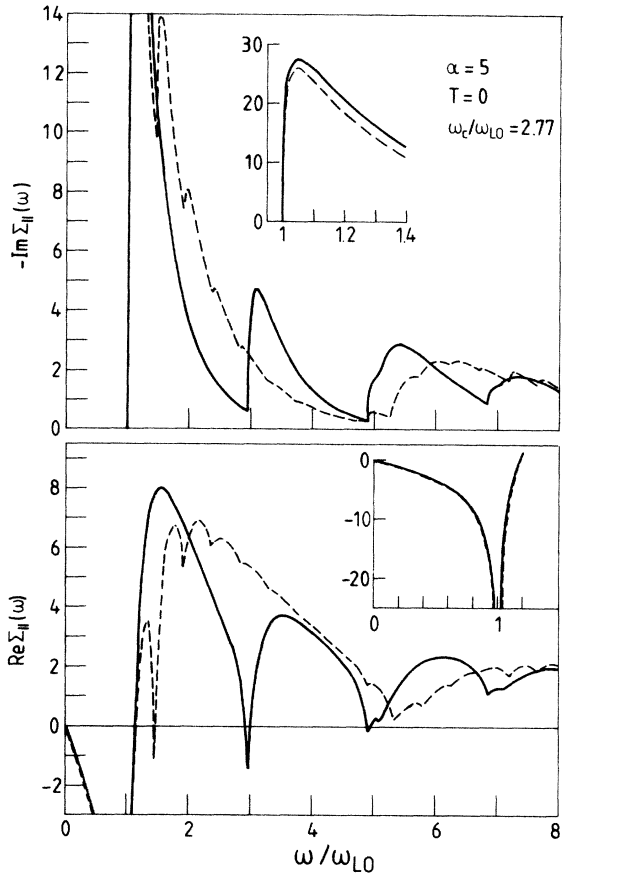

FIG. 12. Real and imaginary part of the memory function for the magneto-optical absorption spectrum of the polaron in the Voigt configuration. Solid and dashed curves correspond to the same polaron state as in Fig. 7.

the intensity (i.e., the oscillator strength) is slightly different as is also apparent from our earlier estimate (Ref. 44). From the polaron cyclotron resonance frequency $\omega_c^*/\omega_{LO}=0.309$ we can deduce a cyclotron mass $m^*/m=\omega_c/\omega_c^*=8.96$ which is different from the Feynman polaron model mass $M_\perp=(v_\perp/w_\perp)^2=5.79$, 1.41 in the dressed and stripped state, respectively. The spectrum for $\omega>\omega_{LO}$ (see Figs. 7, 8, and 11) on the other hand is extremely sensitive to the state in which the polaron is. In the dressed state the magneto-optical absorption spectrum in the Faraday configuration (dashed curve in Figs. 7 and 8) consists of a broad peak (i.e., the "envelope" of the maxima of the dashed curves) originating from a transition to an internal polaron state [which is the relaxed excited peak (RES) (Ref. 33)] with many sharp peaks superimposed. The latter reflect transitions to the different higher Landau levels. The maximum of the broad RES peak is located at $\omega_c/\omega_{LO}\approx 5$ for the Faraday active-mode configuration and at $\omega_c/\omega_{LO}\approx 3$ for the Faraday inactive-mode configuration. In the stripped state the magneto-optical absorption spectrum (solid curves in Figs. 7 and 8) shows a series of well-defined peaks which correspond to transitions to higher Landau levels with the subsequent emission of a LO phonon. With increasing frequency the separation between the peaks decreases and the

width of the peaks increases. This reflects the fact that higher Landau states are more broadened due to the electron-phonon interaction. In the Voigt configuration (Fig. 11) one mainly observes the features of the internal excited polaron states (RES). In the polaron state (dashed curve in Fig. 11) a sharp peak with a broad side band is found which is similar to the absorption spectrum found in the absence of a magnetic field.[30,33] For the state in which, perpendicular to the magnetic field, the polaron is stripped from its phonon cloud, we observe four peaks which probably reflect the different RES.

V. CONCLUSION

In the present paper we have obtained an expression for the magneto-optical absorption spectrum of the Fröhlich polaron which is a natural generalization of the zero-magnetic field expression of the optical-absorption spectrum corresponding to the FHIP approximation,[31] as obtained in Ref. 33 by Devreese *et al.* The present expression is valid for all electron-phonon coupling strength, temperature and magnetic field strength. The perturbation result of Ref. 25 is reobtained in the limit $\alpha \ll 1$.

A limitation of the present approach is due to the divergent behavior of the memory function at several well-defined frequencies. These divergences arise because a zeroth-order model is used which exhibits divergent behavior in the density of states and which, as a consequence, has zeros in the magneto-optical absorption spectrum in the case of the Faraday configuration. For $\alpha \ll 1$ it has been shown that even with these spurious zeros it was possible to obtain reasonable results[25] for the position and width of the cyclotron resonance peak which were in good agreement with experiment.

The question arises how to remedy this deficiency in the theory. One of the possibilities suggested by many authors is to introduce a broadening parameter which is treated as a phenomenological parameter and which results in a density of states which is finite for all energies. In the present paper we did not apply this idea because we do not know how to calculate the broadening parameters from first principles. Using a self-consistent approach[26] it is possible to get rid of the zeros but up to now no numerical results have been published.

An interesting result was obtained concerning the possible polaron instability predicted recently by the present authors.[9] This instability does affect the cyclotron resonance peak only slightly. The dominant change occurs in the magneto-optical absorption spectrum above the LO-phonon threshold which reflects the complicated interaction between the higher Landau levels and the energy levels of the RES. In a recent study, based on fourth-order perturbation theory, Larsen[37] found that in the limit $\alpha \to 0$ and for $\omega_c/\omega_{\mathrm{LO}} > 1.9$, the Feynman polaron theory, applied to the two-dimensional (2D) situation,[38] cannot be variational. Although Larsen's study was restricted to the 2D polaron it shows that we have to be very careful about attaching too much physical significance to the 3D polaron instability of Ref. 9.

ACKNOWLEDGMENTS

This work was partially sponsored by FKFO (Fonds voor Kollektief Fundamenteel Onderzoek), Belgium, Project No. 2.0072.80. One of us (F.M.P.) is grateful to the Nationaal Fund for Scientific Research [Nationaal Fonds voor Wetenschappelijk Onderzoek (NFWO)], Belgium for financial support.

APPENDIX A

In this appendix an alternative representation of the memory function, given in Sec. III, will be derived. This representation clearly reveals the different microscopic scattering processes involved in the present approximation. The basic idea is to perform the time integral analytically (rather than the $\mathbf{k}$ integral as done in Sec. III). Such an approach will lead to an explicit separation of the real and imaginary part of the memory function.

The relaxation function calculated in Sec. III [Eqs. (15), (18), and (19)] can also be written as

$$\Phi_{\mathbf{k}}^{++}(z) = -i \int_0^\infty dt\, e^{izt} \int_0^\beta d\lambda [1+n(\omega_{\mathbf{k}})] e^{-i\omega_{\mathbf{k}}(t-i\lambda)} e^{-k_z^2 D(-t+i\lambda)} e^{-k^2 D_H(-t+i\lambda)}, \tag{A1}$$

where we will expand the exponents so that the integrations (t and λ integration) can be performed explicitly. One has

$$e^{-k_z^2 D(\tau)} = \frac{w_{\parallel}}{v_{\parallel}} \left[\frac{\beta}{2\pi}\right]^{1/2} e^{-k_z^2 a_{\parallel}^2(\beta)} \sum_{n_0, n_0'=0}^{\infty} B_{\parallel}(\beta, n_0, n_0') k_z^{2(n_0+n_0')} \times \int_{-\infty}^{+\infty} dp_z\, e^{-p_z^2/2M_{\parallel}} \exp\left[i\tau \left(\frac{\hbar k_z^2}{2M_{\parallel}} \pm \frac{p_z k_z}{M_{\parallel}} + (n_0 - n_0') s_0 \right) \right], \tag{A2}$$

with

$$a_{\parallel}^2(\beta) = d_0^2 \coth(\beta s_0/2),$$
$$B_{\parallel}(\beta, n_0, n_0') = \frac{1}{n_0!} \{ d_0^2 [1+n(s_0)] \}^{n_0} \times \frac{1}{n_0'!} [d_0^2(s_0)]^{n_0'}, \tag{A3}$$

and similarly

$$e^{-k_{\perp}^2 D_H(\tau)} = e^{-k_{\perp}^2 a_{\perp}^2(\beta)} \prod_{j=1}^{3} \sum_{n_j, n_j'=0}^{\infty} B_j(\beta, n_j, n_j') \times k_{\perp}^{2(n_j+n_j')} e^{i\tau(n_j - n_j')s_j}, \tag{A4}$$

with

$$a_{\perp}^2(\beta)=\sum_{i=1}^{3} d_i^2\coth(\beta s_i/2)\ ,$$

$$B_i(\beta,n_i,n_i')=\frac{1}{n_i'!}\{d_i^2[1+n(s_i)]\}^{n_i} \times\frac{1}{n_i'!}[d_i^2 n(s_i)]^{n_i'}\ . \tag{A5}$$

We introduce the following shorthand notations:

$$\bar{n}=\sum_{i=1}^{3} n_i\ ,$$

$$n_i s^i=\sum_{i=1}^{3} n_i s_i\ , \tag{A6}$$

$$n_\mu s^\mu=\sum_{\mu=0}^{3} n_\mu s_\mu\ ,$$

$$\sum_{n_\mu=0}^{\infty}=\sum_{n_0=0}^{\infty}\sum_{n_1=0}^{\infty}\sum_{n_2=0}^{\infty}\sum_{n_3=0}^{\infty}\ .$$

Inserting the series expansions (A2) and (A4) into the relaxation function (A1) and performing the time integrals we can split up the memory functions [Eqs. (9) and (12)] as follows:

$$\Sigma(z)=\Sigma^M(z)-\Sigma^M(-z)\ ,$$

$$\Sigma_{zz}(z)=\Sigma_{zz}^M(z)-\Sigma_{zz}^M(-z)\ . \tag{A7}$$

For the imaginary part of the memory functions we obtained

$$\mathrm{Im}\Sigma_{zz}^M(\omega)=-\eta(\omega)\sum_{n_\mu,n_\mu'=0}^{\infty} B(\beta,n_\mu,n_\mu')\int_0^\infty du\, E_{\bar{n}+\bar{n}'}([a_{\perp}^2(\beta)/a_{\parallel}^2(\beta)]u)X_{n_0+n_0'}(u,\omega-1-(n_\mu-n_\mu')s^\mu)\ , \tag{A8}$$

with

$$\eta(\omega)=\frac{1}{\omega}\frac{\alpha}{4}\frac{v_{\parallel}}{w_{\parallel}}\left[\frac{\beta}{\pi}\right]^{1/2}\frac{1}{a_{\perp}^2(\beta)}\frac{\sinh(\beta\omega/2)}{\sinh(\beta/2)}\ ,$$

$$B(\beta,n_\mu,n_\mu')=A(\beta,n_\mu,n_\mu')e^{-(\beta/2)(n_\mu-n_\mu')s^\mu}\ ,$$

$$A(\beta,n_\mu,n_\mu')=\prod_{\mu=0}^{3}\frac{1}{n_\mu!}\{h_\mu^2(\beta)[1+n(s_\mu)]\}^{n_\mu}\frac{1}{n_\mu'!}[h_\mu^2(\beta)n(s_\mu)]^{n_\mu'}\ , \tag{A9}$$

$$h_0^2(\beta)=d_0^2/a_{\parallel}^2(\beta);\quad h_i^2(\beta)=d_i^2/a_{\perp}^2(\beta);\quad i=1,2,3$$

and the functions

$$X_n(u,x)=u^n e^{-u}\exp\left[-\frac{\beta}{2}\left[\frac{u}{4a_{\parallel}^2(\beta)M_{\parallel}}+\frac{a_{\parallel}^2(\beta)M_{\parallel}}{u}x^2\right]\right]\ ,$$

$$E_n(x)=\int_0^\infty dt\frac{t^n}{t+x}e^{-t},\quad x\geq 0 \tag{A10}$$

and

$$\mathrm{Im}\Sigma^M(\omega)=-\tfrac{1}{2}\eta(\omega)\sum_{n_\mu,n_\mu'=0}^{\infty} B(\beta,n_\mu,n_\mu')(\bar{n}+\bar{n}')!\int_0^\infty du X_{n_0+n_0'-1}(u,\omega-1-(n_\mu-n_\mu')s^\mu)\ . \tag{A11}$$

The real part of the memory function is given by

$$\mathrm{Re}\Sigma_{zz}^M(\omega)=\rho(\omega)\sum_{n_\mu,n_\mu'=0}^{\infty} A(\beta,n_\mu,n_\mu')\int_{-\infty}^\infty du\, E_{\bar{n}+\bar{n}'}([a_{\perp}^2(\beta)/a_{\parallel}^2(\beta)]u^2)H_{2(n_0+n_0')+1}(u;\omega,1+(n_\mu-n_\mu')s^\mu)\ , \tag{A12}$$

with

$$\rho(\omega)=\frac{1}{\omega}\frac{\alpha}{4\pi}\frac{v_{\parallel}}{w_{\parallel}}\left[\frac{\beta}{\pi}\right]^{1/2}\frac{1+n(\omega_0)}{a_{\parallel}^2(\beta)}\ ,$$

$$H_n(u;\omega,x)=u^n e^{-u^2}\{D((\sqrt{\beta}/u)(u^2-\omega-x))-D((\sqrt{\beta}/u)(u^2-x)) -e^{-\beta x}[D(-(\sqrt{\beta}/u)(u^2+\omega+x))-D(-(\sqrt{\beta}/u)(u^2+x))]\}\ , \tag{A13}$$

where

$$D(x)=\mathrm{P}\int_{-\infty}^{\infty} dt\frac{e^{-t^2}}{t-x}=-2\sqrt{\pi}e^{-x^2}\int_0^x dt\, e^{t^2} \tag{A14}$$

is the Dawson integral (P stands for principal value) and

$$\mathrm{Re}\Sigma^{M}(\omega)=\tfrac{1}{2}\rho(\omega)\sum_{n_\mu,n'_\mu=0}^{\infty}A(\beta,n_\mu,n'_\mu)[(\bar{n}+\bar{n}')!]\int_{-\infty}^{\infty}du\,H_{2(n_0+n'_0)-1}(u;\omega,1+(n_\mu+n'_\mu)s^\mu)\ . \tag{A15}$$

The summations in Eqs. (A8), (A11), (A12), and (A15) reflect the possible internal states which occur before ($\sum_{n'_\mu=0}^{\infty}$) and after ($\sum_{n_\mu=0}^{\infty}$) the emission or absorption of the light quantum $\hbar\omega$.

The limit $T=0$ is of particular interest. In this limit the foregoing expressions simplify considerably because the number of scattering processes is limited (no absorption processes are possible). In the zero-temperature limit Eq. (A8) reduces to

$$\lim_{\beta\to\infty}\mathrm{Im}\Sigma^{M}_{zz}(\omega)=-\frac{\alpha}{\omega}\left[\frac{v_{\|}}{w_{\|}}\right]^3\sum_{n_\mu=0}^{\infty}S(n_\mu)\,|\,C_{n_\mu}(\omega)\,|^{\,n_0+1/2}e^{-R_0^2C_{n_\mu}(\omega)}E_{\bar{n}}(2M_{\|}a_\perp^2C_{n_\mu}(\omega))\Theta(C_{n_\mu}(\omega))\ , \tag{A16}$$

with

$$S(n_\mu)=\prod_{\mu=0}^{3}\frac{R^{2n_\mu}}{n_\mu!}\ ,$$

$$C_{n_\mu}(\omega)=\omega-1-n_\mu s^\mu\ ,$$

where $R_0^2=2M_{\|}d_0=(v_{\|}^2-w_{\|}^2)/v_{\|}w_{\|}^2$; $R_i^2=d_i^2/a_\perp^2$, $i=1,2,3$, $a_\perp^2=\sum_{i=1}^{3}d_i^2=\lim_{\beta\to\infty}a_\perp^2(\beta)$, and $\Theta(x)=0$ $(x<0)$, $1(x>0)$. Similarly Eq. (A11) becomes

$$\lim_{\beta\to\infty}\mathrm{Im}\Sigma^{M}(\omega)=-\frac{1}{\omega}\frac{\alpha}{4}\frac{v_{\|}}{w_{\|}}\frac{1}{a_\perp^2}\sum_{n_\mu=0}^{\infty}S(n_\mu)(\bar{n}!)\,|\,C_{n_\mu}(\omega)\,|^{\,n_0-1/2}e^{-R_0^2C_{n_\mu}(\omega)}\Theta(C_{n_\mu}(\omega))\ . \tag{A17}$$

The real parts of the memory functions simplify to

$$\lim_{\beta\to\infty}\mathrm{Re}\Sigma^{M}_{zz}(\omega)=\frac{1}{\omega}\frac{\alpha}{\pi\sqrt{2}}\frac{M_{\|}}{d_0}\sum_{n_\mu=0}^{\infty}\frac{S(n_\mu)}{R_0^{2n_0}}\int_{-\infty}^{\infty}du\,u^{2(n_0+1)}e^{-u^2}$$
$$\times E_{\bar{n}}[(a_\perp^2/d_0^2)u^2]\left[\frac{1}{u^2-R_0^2C_{n_\mu}(0)}-\mathrm{P}\left[\frac{1}{u^2-R_0^2C_{n_\mu}(\omega)}\right]\right]\ , \tag{A18}$$

$$\lim_{\beta\to\infty}\mathrm{Re}\Sigma^{M}(\omega)=\frac{1}{\omega}\frac{\alpha}{2\pi\sqrt{2}}\frac{d_0M_{\|}}{a_\perp^2}\sum_{n_\mu=0}^{\infty}\frac{S(n_\mu)}{R_0^{2n_0}}(\bar{n}!)\int_{-\infty}^{\infty}du\,u^{2n_0}e^{-u^2}\left[\frac{1}{u^2-R_0^2C_{n_\mu}(0)}-\mathrm{P}\left[\frac{1}{u^2-R_0^2C_{n_\mu}(\omega)}\right]\right]\ . \tag{A19}$$

APPENDIX B

Explicit analytic expressions will be given for the different memory functions in the limit of small electron-phonon coupling strength. The results of perturbation theory as given in Refs. 21 and 25 are reobtained. But the present analytic expressions are simpler in the sense that we were able to perform explicitly a number of summations which appears in the results of Refs. 21 and 25.

We refer to the results of Appendix A and take the limit $\alpha\to0$ which amounts to $v_{\|}/w_{\|}\to1$, $v_\perp/w_\perp\to1$ and which results in $s_0=s_1=s_2$, $s_3\to\omega_c$, $d_0=d_1=d_2=0$, $d_3^2\to1/2\omega_c$, $a_{\|}^2(\beta)\to0$, $a_\perp^2(\beta)\to2\omega_c\tanh(\beta\omega_c/2)$. This results in (the same notations are used as in Appendix A)

$$\lim_{\alpha\to0}\left[\frac{1}{\alpha}\mathrm{Im}\Sigma^{M}_{zz}(\omega)\right]=\frac{-1}{\omega}\frac{\sqrt{\beta}}{2\sqrt{\pi}}\frac{\sinh(\beta\omega/2)}{\sinh(\beta/2)}\sum_{n,n'=0}^{\infty}\frac{[2\cosh(\beta\omega_c/2)]^{-(n+n')}}{n!n'!}$$
$$\times\int_0^{\infty}dx\,E_{n+n'}\left[\frac{x}{\omega_c\tanh(\beta\omega_c/2)}\right]$$
$$\times\exp\left[-\frac{\beta}{2x}[\omega-1-(n-n')\omega_c]^2-\frac{\beta}{4}x\right]\ , \tag{B1}$$

$$\lim_{\alpha\to0}\left[\frac{1}{\alpha}\mathrm{Im}\Sigma^{M}(\omega)\right]=-\frac{1}{\omega}\frac{\sqrt{\beta}}{2\sqrt{\pi}}\frac{\sinh(\beta\omega/2)}{\sin(\beta/2)}\omega_c\tanh\left[\frac{\beta\omega_c}{2}\right]$$
$$\times\sum_{n,n'=0}^{\infty}\frac{(n+n')!}{(n!)(n'!)}\left[2\cosh\left[\frac{\beta\omega_c}{2}\right]\right]^{-(n+n')}K_0(\tfrac{1}{2}\beta\,|-\omega+1+(n-n')\omega_c\,|)\ , \tag{B2}$$

with $K_0(x)$ the Bessel function of imaginary argument of order zero,

$$\lim_{\alpha\to 0}\left[\frac{1}{\alpha}\mathrm{Re}\Sigma^{M}_{zz}(\omega)\right]=\frac{1}{\omega}\frac{\sqrt{\beta}}{2\pi\sqrt{\pi}}[1+n(\omega_0)]\sum_{n,n'=0}^{\infty}\frac{e^{(\beta/2)(n-n')\omega_c}}{(n!)(n'!)[2\cosh(\beta\omega_c/2)]^{n+n'}}$$
$$\times\int_{-\infty}^{\infty}du\,uE_{n+n'}(u^2/[\omega_c\tanh(\beta\omega_c/2)])H_1(u;\omega,1+(n-n')\omega_c)\,, \tag{B3}$$

$$\lim_{\alpha\to 0}\left[\frac{1}{\alpha}\mathrm{Re}\Sigma^{M}(\omega)\right]=-\frac{1}{\omega}\frac{\sqrt{\pi\beta}}{4}\frac{\omega_c\tanh(\beta\omega_c/2)}{\sinh(\beta/2)}$$
$$\times\sum_{n,n'=0}^{\infty}\frac{(n+n')!}{(n!)(n'!)}\left[2\cosh\left[\frac{\beta\omega_c}{2}\right]\right]^{-(n+n')}$$
$$\times\{-I_0(\tfrac{1}{2}\beta|1+(n-n')\omega_c|)+e^{\beta\omega/2}I_0(\tfrac{1}{2}\beta|-\omega+1+(n-n')\omega_c|)$$
$$\times\Theta(-\omega+1+(n-n')\omega_c)+e^{\beta\omega/2}I_0(\tfrac{1}{2}\beta|-\omega-1+(n-n')\omega_c|)$$
$$\times\Theta(-\omega-1+(n-n')\omega_c)\}\,, \tag{B4}$$

with $I_0(x)$ a Bessel function of imaginary argument.

In the limit of $T=0$ the above expressions simplify to

$$\lim_{\beta\to\infty}\lim_{\alpha\to 0}\frac{\mathrm{Im}\Sigma^{M}_{zz}(\omega)}{\alpha}=\frac{-1}{\omega}\sum_{n=0}^{\infty}\frac{1}{n!}[\omega-(1+n\omega_c)]^{1/2}E_n([\omega-(1+n\omega_c)]/\omega_c)\Theta(\omega-(1+n\omega_c))\,, \tag{B5}$$

$$\lim_{\beta\to\infty}\lim_{\alpha\to 0}\frac{\mathrm{Im}\Sigma^{M}(\omega)}{\alpha}=-\frac{\omega_c}{2\omega}\sum_{n=0}^{\infty}\frac{\Theta(\omega-(1+n\omega_c))}{[\omega-(1+n\omega_c)]^{1/2}}\,, \tag{B6}$$

$$\lim_{\beta\to\infty}\lim_{\alpha\to 0}\frac{\mathrm{Re}\Sigma^{M}_{zz}(\omega)}{\alpha}=\frac{1}{\omega}\sum_{n=0}^{\infty}\frac{1}{n!}\{(\omega_c)^{1/2}[G_{n+1/2}((1+n\omega_c)/\omega_c)-G_{n+1/2}((1+n\omega_c-\omega)/\omega_c)]$$
$$-(1+n\omega_c)^{1/2}G_n((1+n\omega_c)/\omega_c)+(1+n\omega_c-\omega)^{1/2}$$
$$\times G_n((1+n\omega_c-\omega)/\omega_c)\Theta(1+n\omega_c-\omega)\}\,, \tag{B7}$$

where we defined the function

$$G_\mu(x)=\mathrm{P}\int_0^\infty dt\frac{t^\mu e^{-t}}{t-x} \tag{B8}$$

and

$$\lim_{\beta\to\infty}\lim_{\alpha\to 0}\frac{\mathrm{Re}\Sigma^{M}(\omega)}{\omega}=\frac{\omega_c}{2\omega}\sum_{n=0}^{\infty}\left[\frac{1}{(1+n\omega_c)^{1/2}}-\frac{\Theta(1+n\omega_c-\omega)}{(1+n\omega_c-\omega)^{1/2}}\right]. \tag{B9}$$

---

*Also at University of Antwerp, Rijksuniversitair Centrum Antwerpen, B-2020 Antwerpen, Belgium and at Eindhoven University of Technology, NL-5600 MB Eindhoven, The Netherlands.

[1]R. W. Hellwarth and P. M. Platzman, Phys. Rev. **128**, 1599 (1962).

[2]D. M. Larsen, Phys. Rev. **135**, A419 (1964); in *Polarons in Ionic Crystals and Polar Semiconductors*, edited by J. T. Devreese (North-Holland, Amsterdam, 1972), p. 237.

[3]K. K. Bajaj, Phys. Rev. **170**, 694 (1968); Nuovo Cimento B **55**, 244 (1968).

[4]M. Porsch, Phys. Status Solidi **41**, 151 (1970).

[5]R. Evrard, E. Kartheuser, and J. Devreese, Phys. Status Solidi **41**, 431 (1970).

[6]E. Kartheuser and R. Negrete, Phys. Status Solidi B **57**, 77 (1973).

[7]Y. Lépine and D. Matz, Can. J. Phys. **54**, 1979 (1976); Y. Lépine, J. Phys. C **18**, 1817 (1985).

[8]M. Saitoh, J. Phys. Soc. Jpn. **49**, 886 (1980); **50**, 2295 (1981); K. Arisawa and M. Saitoh, Phys. Lett. **82A**, 462 (1980).

[9]F. M. Peeters and J. T. Devreese, Solid State Commun. **39**, 445 (1981); Phys. Rev. B **25**, 7281 (1982); **25**, 7302 (1982).

[10]R. P. Feynman, Phys. Rev. **97**, 660 (1955).

[11]V. L. Gurevich and Yu. A. Firsov, Zh. Eksp. Teor. Fiz. **40**, 198 (1961) [Sov. Phys.—JETP **13**, 137 (1961)].

[12]V. Gurevich, I. Lang, and Y. Firsov, Fiz. Tverd. Tela (Leningrad) **4**, 1252 (1962) [Sov. Phys.—Solid State **4**, 918 (1962)].

[13]R. Kubo, S. J. Miyake, and N. Hashitsume, Solid State Phys. **17**, 269 (1965).

[14]E. Johnson and D. Larsen, Phys. Rev. Lett. **16**, 655 (1966).

[15]P. Harper, Proc. Phys. Soc. **92**, 793 (1967).
[16]L. I. Korovin and S. T. Tavlov, Zh. Eksp. Teor. Fiz. **6**, 525 (1967) [Sov. Phys.—JETP **26**, 979 (1968)].
[17]M. Nakayama, J. Phys. Soc. Jpn. **27**, 636 (1969).
[18]R. Enck, A. Saleh, and H. Fan, Phys. Rev. **182**, 790 (1969).
[19]P. Harper, J. Hodby, and R. Stradling, Rep. Prog. Phys. **36**, 1 (1973).
[20]R. Kaplan and K. L. Ngai, Comm. Solid State Phys. **5**, 157 (1973); **6**, 17 (1974); **6**, 23 (1974).
[21]J. Van Royen, J. De Sitter, L. F. Lemmens, and J. T. Devreese, Physica (Utrecht) **81B&C**, 101 (1977).
[22]J. P. Vigneron, R. Evrard, and E. Kartheuser, Phys. Rev. B **18**, 6930 (1978).
[23]J. T. Devreese, in *Theoretical Aspects and New Developments in Magneto-Optics,* edited by J. T. Devreese (Plenum, New York, 1980), p. 217.
[24]J. T. Devreese, J. De Sitter, E. J. Johnson, and K. L. Ngai, Phys. Rev. B**17**, 3207 (1981).
[25]J. Van Royen and J. T. Devreese, Solid State Commun. **40**, 947 (1981); J. Van Royen, J. De Sitter, and J. T. Devreese, Phys. Rev. B **30**, 7154 (1984).
[26]K. K. Thornber, Phys Rev. B **3**, 1929 (1971); **4**, 675E (1971).
[27]K. K. Thornber, in *Path Integrals and their Applications in Quantum, Statistical and Solid State Physics,* edited by G. J. Papadopoulos and J. T. Devreese (Plenum, New York, 1978), p. 359.
[28]M. Saitoh, J. Phys. C **15**, 6981 (1982); J. Phys. A **16**, 1795 (1983).
[29]H. Mori, Prog. Theor. Phys. **33**, 423 (1965); **34**, 399 (1965).
[30]F. M. Peeters and J. T. Devreese, Phys. Rev. B **28**, 6051 (1983).
[31]R. P. Feynman, R. W. Hellwarth, C. K. Iddings, and P. M. Platzman, Phys. Rev. **127**, 1004 (1962).
[32]P. M. Platzman, in *Polarons and Excitons,* edited by G. C. Kuper and G. D. Whitfield (Oliver and Boyd, Edinburgh, 1963), p. 123.
[33]J. Devreese, J. De Sitter, and M. Goovaerts, Phys. Rev. B **5**, 2367 (1972); and J. T. Devreese, in *Polarons in Ionic Crystals and Polar Semiconductors,* edited by J. T. Devreese (North-Holland, Amsterdam, 1972), p. 83.
[34]R. Kubo, J. Phys. Soc. Jpn. **21**, 570 (1957).
[35]W. Götze and K. H. Michel, in *Dynamical Properties of Solids,* edited by G. K. Horton and A. A. Maradudin (North-Holland, Amsterdam, 1974).
[36]D. Foster, *Hydrodynamic Fluctuations, Broken Symmetry, and Correlation Functions* (Benjamin, New York, 1975).
[37]D. M. Larsen, Phys. Rev. B **32**, 2657 (1985).
[38]Wu Xiaoguang, F. M. Peeters, and J. T. Devreese, Phys. Rev. B **32**, 7964 (1985).
[39]J. T. Devreese and F. M. Peeters, Solid State Commun. **58**, 861 (1986).
[40]G. Lindemann, R. Lassnig, W. Seidenbusch, and E. Gornik, Phys. Rev. B **28**, 4693 (1983).
[41]F. M. Peeters and J. T. Devreese, Physica (Utrecht) **127B**, 408 (1984).
[42]J. Waldman, D. Larsen, P. Tannenwald, C. Bradley, D. Cohn, and B. Lax, Phys. Rev. Lett. **23**, 1033 (1969).
[43]J. W. Hodby, G. P. Russell, F. M. Peeters, J. T. Devreese, and D. Larsen (unpublished).
[44]F. M. Peeters and J. T. Devreese, in *Proceedings of the Conference on Application of High Magnetic Fields in Semiconductor Physics,* edited by G. Landwehr (Springer-Verlag, Berlin, 1983), p. 406.